39th AIAA Thermophysics Conference, 25-28 June 2007, Miami

Direct Numerical Simulation of Turbulent Multispecies Channel Flow with Wall Ablation

O. Cabrit * and L. Artal †

CERFACS, 31057 Toulouse Cedex 01, France ,

F. Nicoud ‡

Université Montpellier II, 34095 Montpellier, France

The design of solid rocket motors requires the prediction of changes induced by the ablation process occurring at the nozzle throat. The present study aims at understanding the effects of ablation on the turbulent boundary layer performing direct numerical simulations in a channel flow configuration. An ablation boundary condition for arbitrary chemical composition and pyrolysis scheme is developed and presented in this paper. Then, two DNS of a seven species reacting flow are performed: a) with inert walls; b) with ablated walls. Generated data are compared and analyzed looking at first order statistics. It is shown that the classical law of the wall for velocity and temperature are not appropriate to represent the numerical result. The chemical equilibrium assumption is shown to be valid in the inert case and a wall function consistent with this assumption is in fair agreement with the results.

Nomenclature

$\dot{m}$	wall mass flux, $kg \cdot m^{-2} \cdot s^{-1}$
$\dot{r}_c$	carbon surface recession rate, m/s
$\dot{s}_k$	surface production rate of k, $kg \cdot m^{-2} \cdot s^{-1}$
$\mathcal{D}_k$	equivalent diffusion coefficient of species k into the rest of the mixture
$\mathcal{D}_{ij}$	binary diffusion coefficient of species i into j
$\mathcal{Q}$	progress rate of the heterogeneous reaction, $mol \cdot m^{-2} \cdot s^{-1}$
ν	kinematic viscosity
ν_k	$= \nu_k^b - \nu_k^f$, global stoichiometric coefficient of species k
ρ	mass density
τ_w	wall shear stress
C_p	heat capacity at constant pressure
C_v	heat capacity at constant volume
h	channel half-width
p	thermodynamic pressure
Pr	Prandtl number
q_w	wall heat flux
R	perfect gas constant
Re_τ	$= u_\tau h/\nu_w$, friction Reynolds number
Sc_k	Schmidt number of species k
T	temperature
T^+	$= (T_w - T)/T_\tau$, temperature in wall units
T_τ	$= q_w/(\rho_w\, C_{p,w}\, u_\tau)$, friction temperature
U^+	$= u/u_\tau$, velocity in wall units
u_τ	$= \sqrt{\tau_w/\rho_w}$, friction velocity
V^{cor}	correction velocity for the Hirschfelder and Curtiss approximation
V_{inj}	pyrolysis gas injection velocity
V_k	diffusion velocity of species k
W	mean molecular weight of the mixture
W_k	molecular weight of species k
X_k	mole fraction of species k
Y_k	mass fraction of species k

Subscripts

n	in the wall normal direction
w	evaluated at wall

Conventions

$\langle\cdot\rangle$	space average operator
$\nabla\cdot$	gradient operator
$\overline{\cdot}$	time average operator

Superscripts

$+$	expressed in viscous wall units scaling
t	evaluated at time t
$t+1$	evaluated at time $t + \Delta t$

*Ph.D. student, CERFACS, CFD Team, 42 avenue Gaspard Coriolis; olivier.cabrit@cerfacs.fr

†Ph.D., former Ph.D. student at CERFACS, currently at ONERA/DMAE; lea.artal@onecert.fr

‡Professor, Université Montpellier 2, I3M - CNRS UMR 5149 - CC51; franck.nicoud@univ-montp2.fr

I. Introduction

Ablation process has been studied for different space applications with several different approaches for more than forty years.[1] Modeling universal ablation requires knowledges and expertise in diverse disciplines such as chemistry and multispecies physics, multi-phase flow dynamics, thermo-structural mechanics of composite materials, physics of particle/droplet impacts, rugosity interaction mechanisms, or physics of radiation heat transfer. Despite huge scientific research efforts, a unique model able to describe the whole complexity of this phenomenon does not exist. It is thus essential to properly define the framework of each investigation in order to define appropriated simplifications.

The use of high energy propellants in Solid Rocket Motors (SRM) requires to understand the thermophysics interacting between structural components and high energy fluids. Carbon-carbon composites are widely used for SRM nozzle structure design and exposed to severe thermochemical attack which can lead to an ablation process at the gas/solid interface. Pyrolysis processes occur inside the C/C composite material due to oxidizing species such as H_2O and CO_2, and the nozzle surface starts to recede. This recession behavior is an issue during motor firing because the performance of SRM is lowered by the increase of the throat area and the nozzle surface roughness. Therefore, the ablation process must be estimated and incorporated into the motor design. Full-scale motor firings are very expensive and does not provide sufficient information to understand the whole phenomenon. For economical and efficiency reasons, the use of accurate numerical models is rather preferred to design SRM nozzles.

Many studies have already proposed to couple numerically the gaseous phase and the solid structure.[2–5] However, most of them are dedicated to the structural material characterization by predicting the recession rate or the surface temperature and few are oriented towards the fluid characterization. Hence, the objective of the present study is to support the development of industrial numerical methods by understanding the changes induced in the turbulent boundary layer when ablation occurs. Indeed, the boundary layer structure is expected to be modified because the heat and mass balances at the gas/solid interface depend on the heterogeneous reactions.

This work is motivated by the use of Reynolds Averaged Navier-Stokes (RANS) methods in industrial design codes. Indeed, to save CPU time, these RANS codes are coupled with wall laws to assess the mass/momemtum/energy fluxes at the solid boundaries. The classical logarithmic law is commonly implemented and provides reasonable results for simple incompressible flows. The trend today is to generalize this wall law to account for more physics including strong changes of density due to high temperature gradients and multispecies reacting flow specificities. The purpose here is to analyze detailed relevant data to support the development of wall functions able to predict reliable wall fluxes (i.e. the wall shear stress τ_w and the wall heat flux q_w) when ablation happens.

This study aims at presenting the results obtained performing two types of DNS. The first one is a DNS of turbulent reacting multispecies channel flow with quasi-isothermal inert walls. It constitutes a reference DNS for the second one which simulates the same fluid under the same operating conditions with quasi-isothermal ablative walls. For simplification reasons, the questions of two-phase flow effects and mechanical erosion will not be discussed in the present work even if recent studies have shown the strong influence of these phenomena.[6,7] A reacting gaseous phase model is merely coupled with a termochemical ablated wall boundary condition.

The first section of the paper presents the solver and the numerical strategy followed to set up the DNS. Particular attention is given to the description of the boundary conditions and notably to the quasi-isothermal ablated wall boundary condition specifically developed for this work. First order statistics are then analyzed in the second part.

II. Solver and Numerical Strategy

II.A. Description of the Code

II.A.1. Basic Concepts

DNS were performed with the solver AVBP[8] developed at CERFACS. This parallel code offers the capability to handle structured, unstructured, or hybrid grids in order to solve the full 3D compressible reacting Navier-Stokes equations. AVBP is thus mainly dedicated to the prediction of unsteady turbulent reacting flows in

complex geometries. During the past years, the efficiency of AVBP has been widely demonstrated[a] with both large eddy simulations (LES) and direct numerical simulations (DNS).

In this work, the flow solver used for the discretization of governing equations is based on the cell-vertex finite element method for arbitrary elements. The TTGC scheme[9] specifically conceived for unsteady flows computations is employed. This is a Taylor-Galerkin third-order accurate scheme in both time and space with an explicit multistage Runge-Kutta time-stepping for temporal integration.

II.A.2. Governing Equations

The conservation equations for three dimensional turbulent, compressible, reacting gaseous flows are well-known, and several authors have yet described their derivation.[10] The code solves the continuity equation, the three dimensional momentum conservation equations, the energy conservation equation and as many species conservation equations as there are species in the simulated mixture. Besides, the following assumptions are used to close the problem:

- radiation heat transfer is negligible,
- the fluid is assumed to be an ideal gas,
- the viscosity is power-law temperature dependent,
- constant Prandtl (Pr) and species Schmidt numbers (Sc_k),
- the classical Arrhenius law models the chemical reaction kinetics,
- no Soret and Dufour effects involved in multispecies diffusion,
- the Hirschfelder and Curtiss approximation[11] with correction velocity is used to evaluate diffusion velocities of each species.

As mentioned by Giovangigli[12] the last approximation is the best first-order accurate model for estimating diffusion velocities of a multicomponent mixture. The rigorous inversion of the diffusion velocity system can then be replaced by a simpler one:

$$V_k X_k = -\mathcal{D}_k \nabla X_k \tag{1}$$

where $\mathcal{D}_k$ is an equivalent diffusion coefficient of species k into the rest of the mixture. It is built from the binary diffusion coefficients $\mathcal{D}_{ij}$ which can be assessed from the gas kinetic theory:[12]

$$\mathcal{D}_k = \frac{1 - Y_k}{\sum_{j \neq k} X_j / \mathcal{D}_{jk}} \tag{2}$$

Mass conservation is a specific issue when dealing with reacting flows. To insure that the system of equations satisfies the two constraints $\sum_k Y_k = 1$ and $\sum_k Y_k V_k = 0$, a correction velocity V^{cor} is added to the convection velocity in the species conservation equations. At each time step, the correction velocity is computed so that:

$$V^{cor} = \sum_k \mathcal{D}_k \frac{W_k}{W} \nabla X_k \tag{3}$$

with W and W_k the molecular weight of the mixture and of each species k, respectively.

Combined with the assumption of constant Schmidt numbers, the Hirschfelder and Curtiss approximation is very convenient because the equivalent diffusion coefficients can be easily related to the kinematic viscosity according to: $\mathcal{D}_k = \nu / Sc_k$. The problem is then closed by imposing the Schmidt numbers and it is not necessary to compute the $\mathcal{D}_{ij}$ coefficients which are complex functions of collision integrals and thermodynamics variables.

Note that if the the mixture contains only two species, the system Eq. (1) is reduced to the classical Fick's law which is exact for a binary mixture with no pressure gradient and no volume forces. However, in all other cases and especially in the present one where the mixture is composed of seven species, the Hirschfelder and Curtiss approximation differs from the Fick's law. Hence, the present DNS provide results with an improved diffusion model compared to the work of Kendall, Rindal and Bartlett[5] in which a Fick's law with the Bird approximation for binary diffusion coefficients is assumed.

[a] http://www.cerfacs.fr/cfd/CFDPublications.html

II.B. Operating Conditions of the DNS

Thermodynamics

The thermodynamic operating conditions of the simulations represent the ones that occur inside the nozzle convergent of the Ariane 5 P230 solid rocket motor. Table 1 gathers a few data used to settle the DNS. From left to right: the thermodynamic pressure p, the wall temperature T_{wall}, the mean temperature inside the domain T_{mean} and the Mach number. Note that the flow is subsonic and compressibility effects can thus be neglected.

Table 1. Thermodynamic operating conditions

$\mathbf{p}$	$\mathbf{T_{wall}}$	$\mathbf{T_{mean}}$	**Mach**
$10\ MPa$	$2700\ K$	$3000\ K$	0.2

Equivalent mixture and kinetics

Realistic gas ejected from this kind of nozzle contains about a hundred gaseous species. Only the species whose molar fraction is greater than 0.001 have been kept in this study. A simpler mixture composed of seven species is then generated, nitrogen being used as a diluent. Usual values of transport properties are given by the EGLIB library.[13] Prandtl number of the equivalent mixture is equal to 0.47 and the Schmidt numbers of each retained species are given in table 2.

Table 2. Schmidt numbers of the equivalent mixture

species	$\mathbf{H_2}$	**H**	$\mathbf{H_2O}$	**OH**	$\mathbf{CO_2}$	**CO**	$\mathbf{N_2}$
$\mathbf{Sc_k}$	0.20	0.15	0.65	0.53	0.98	0.86	0.87

This equivalent mixture then needs a reliable kinetic scheme which reproduces the concentration changes of each species during the simulations. Thereby, a kinetic scheme based on seven chemical reactions has been tuned using the GRI-Mech[b] elementary equations. It has been validated verifying that an AVBP computation with this reduced kinetic scheme is able to predict the right chemical equilibrium composition given by the EQUIL library of the CHEMKIN[c] software and the whole set of species involved in GRI-Mech chemical reaction mechanism.

The experiments of Geisler[14] and Cvelbar[15] as well as the numerical analysis of Keswani, Andiroglu, Campbell and Kuo[16] have revealed the strong influence of aluminum on C/C composite ablation process. Indeed, the recession rate decreases when aluminum concentration increases and the presence of aluminum component could thus be expected in the simulated equivalent mixture. However, the purpose of the present work is not to show up such a behavior on ablation process. The development of a kinetic scheme involving aluminum species ask a stronger effort which is not necessary here. The same equivalent mixture and kinetic scheme (without aluminum) are thus used in both inert and ablated walls simulations.

II.C. Computational Domain and Numerical Resolution

The same computational domain is used for both inert and ablated walls simulations. The flow geometry and the coordinate system are shown in figure 1.

Periodic boundary conditions are applied in the homogeneous streamwise (x) and spanwise (z) directions and the pressure gradient that drives the flow is enforced by adding a space and time constant source term to the momentum conservation equation. A source term that warms the fluid in volume is also added to the energy equation in order to sustain the mean temperature inside the computational domain. This energy source term is applied as a space constant and adjusted dynamically at each time step according to:

$$\mathcal{S}_{energy}^{t+1} = \overline{\langle\rho\rangle}\ \overline{\langle C_v\rangle}\ \frac{T_{mean} - \langle T\rangle^t}{\tau_{relax}} \tag{4}$$

where $\mathcal{S}_{energy}^{t+1}$ denotes the energy source term at time $t + \Delta t$, $\langle T\rangle^t$ the space average temperature at time t, T_{mean} the target operating temperature to reach and τ_{relax} a relaxation time constant. In this work, τ_{relax} has been chosen to be about one third of the characteristic diffusion time, $\tau_{diffusion} = \frac{h}{u_\tau}$.

[b] http://www.me.berkeley.edu/gri_mech

[c] Software tool developed at Sandia National Laboratories for solving complex chemical kinetics problems.

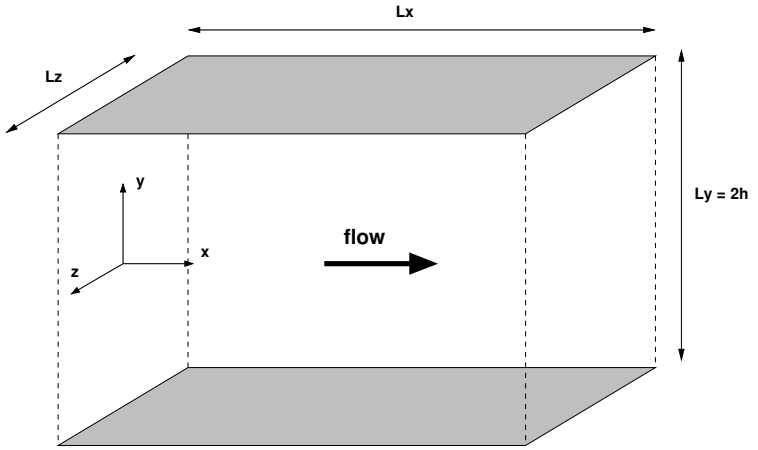

Figure 1. Sketch of a computational domain

The original Kim, Moin and Moser[17] channel calculation at $Re_\tau = 180$ was at low Reynolds number. Several studies[18] have later shown that it was necessary to simulate channel flows in wider boxes to account for turbulent structures of high Reynolds number wall-bounded flows and to expect a sufficiently large log layer. Hence, the value of $Re_\tau = 300$ has been retained in the present work. This corresponds to a Reynolds number of $Re = 5700$, based on the centerline mean velocity, the channel half-width and the kinematic viscosity at the wall. Computations were carried out with tetrahedral elements and $192,231$ grid points ($31 \times 159 \times 39$, in x, y, z). The x and z grid spacing in viscous wall units[d] is $\Delta x^+ \approx 30$ and $\Delta z^+ \approx 9.5$. In the wall-normal direction, the first point off the wall is at $y^+ \approx 0.85$, the maximum y grid spacing is $\Delta y^+_{max} \approx 6.2$, and the first 9 grid points are below $y^+ = 10$. Table 3 summarizes the parameters of the present simulations.

Table 3. Computational domain and numerical resolution

DNS	$\mathbf{Re}_\tau$	**h** (mm)	$\mathbf{L_x/h}$	$\mathbf{L_z/h}$	Δx^+	Δz^+	Δy^+_{max}	$\mathbf{V^+_{inj}}$
inert	300	0.198	π	$0.4\,\pi$	≈ 30	≈ 9.5	≈ 6.2	0
	homogeneous directions: x, z, t							
ablation	300	0.198	π	$0.4\,\pi$	≈ 30	≈ 9.5	≈ 6.2	0.0035
	homogeneous directions: x, z							

The values of Re_τ and the normalized domain size lenghts L_x/h and L_z/h seem to be very small compared to the recent simulation of Hoyas an Jiménez.[19] However, the goal here is not to provide high-order turbulence statistics and this is why the domain was built to be about twice wider than the minimal unit flow conditions defined by Jiménez and Moin.[20] In addition, the multicomponent reacting DNS of Artal and Nicoud[21] has demonstrated that relevant data can be obtained with such a computational domain.

Note that for the ablation case, heterogeneous reactions induce a recession behavior which is modeled by imposing the normal injection velocity, V_{inj} (see paragraph II.D.2 where this question is discussed). As a consequence, the mean mass density increases and the solution is not statistically steady. Therefore, statistical averages are assessed over the homogeneous x and z directions only and not over time.

II.D. Boundary Conditions

Wall boundary conditions distinguish the two types of DNS performed in this study. On the one hand, inert walls are simulated applying a no-slip quasi-isothermal boundary condition that conserves the average mass density all along the simulation. On the other hand, a new boundary condition for ablated walls is developed and integrated inside the code. Forthcoming sections clearly describe these two kinds of boundary conditions.

[d]Quantities with superscript $^+$ are normalized by friction quantities, e.g. dimensions are scaled by $\frac{\nu_w}{u_\tau}$ and velocities by u_τ.

II.D.1. Inert Walls

With a classical no-slip isothermal wall boundary condition, the wall temperature is imposed with a Dirichlet condition. It is known that such a hard constraint induces slight drifts on the mean pressure and the mean mass density. However slight these changes are, a DNS in channel flow configuration is very sensitive to this kind of boundary condition and a non-negligible discrepancy exists after numerous iterations. For instance in the inert walls DNS, around $3,000,000$ iterations are needed between the initial condition and the statistically steady state of the simulation (i.e. when the profile of total shear stress is linear and the total kinetic energy is quasi-constant) and 600,000 more to achieve the statistical treatment. This discrepancy influences the results in two ways: a) the target operating conditions are not sustained all along the simulations and b) the variation of mean pressure and mass density weakly distort the statistics.

To avoid this undesired behavior, a boundary condition that preserves the mean mass density has been developed. It is based on a Neumann like condition strategy, i.e. the wall normal heat flux $q_{w,n}$ is imposed rather than a sharp value of the wall temperature. Then, the numerical scheme predicts the wall temperature. For each boundary node, knowing the wall node temperature T_w^t at time t, the value of $q_{w,n}^{t+1}$ at time $t + \Delta t$ is explicited and calculated as follow:

$$q_{w,n}^{t+1} = \frac{T_w^{target} - T_w^t}{R_{relax}} \tag{5}$$

where, T_w^{target} is the target wall temperature (e.g. $2700K$ in the present work) and R_{relax} a resistance like relaxation coefficient which is adapted so that the wall is quasi-isothermal during the simulation. The tangential components of q_w are predicted by the scheme and left unchanged. Although this formulation cannot provide the strictly required temperature everywhere on the wall at any time step, the variations of temperature stay smooth and low ($\Delta T_w \approx \pm 5K$). Concerning the no-slip aspect of this boundary condition, a zero velocity condition is merely applied on the wall by the hard way.

II.D.2. Ablated Walls

The goal here is to model the recession behavior associated with thermochemical ablation at quasi-constant temperature (no mechanical erosion is considered). Sublimation and vaporization of carbon component are not taken into account in this boundary condition. Indeed, the code only solves the gaseous phase and the analysis that follows does not claim to predict the behavior of the nozzle solid material. Such a material characterization would need to perform a full DNS that would solve the gaseous phase and the solid phase by a coupling way. In this case solely, a boundary condition that would be able to take into account the pyrolysis and the sublimation phenomena should be required. Moreover, the ablation process is simplified with the same assumption used by Baiocco and Bellomi,[3] namely the pyrolysis gas velocity is assumed to be orthogonal to the receding surface.

Hence, this new boundary condition prescribes three quantities to mimic the behavior of an ablated wall: T_w the temperature at the wall, V_{inj} the normal pyrolysis gas injection velocity, and $\nabla_n Y_{k,w}$ the normal mass fraction flux of each species involved in the heterogeneous reactions.

The boundary condition is inspired by the wall recession model proposed by Keswani and Kuo[2,16] and the work of Kendall, Rindal and Bartlett.[5] Starting from the conservation equation of the wall mass flux $\dot{m}$, one can write:

$$\dot{m} = \rho_c \dot{r}_c = \rho_w V_{inj} \tag{6}$$

where ρ_c denotes the mass density of the composite material, $\dot{r}_c$ the recession rate of the solid surface, ρ_w the mass density of the pyrolysis gas generated by the heterogeneous reactions (i.e. the mass density of the mixture at the wall) and V_{inj} the normal injection velocity. The code only solves the gaseous phase and that is why the equality $\dot{m} = \rho_w V_{inj}$ is the only interesting part of Eq. (6). Thereby, the species mass flux at the wall $\dot{m} Y_{k,w}$ can be expressed and the mass species balance at the interface is projected onto the wall normal direction and written for each k species:

$$\rho_w Y_{k,w} \left(V_{inj} + V_{k,n} \right) = \dot{s}_k \tag{7}$$

where $\dot{s}_k$ is the surface production rate of species k that depends on the chemical heterogeneous reactions involved in the pyrolysis process (the modeling of $\dot{s}_k$ is presented further in this section). By summing

over all the species, and according to the mass conservation constraint $\sum_k Y_k V_k = 0$, an expression for the injection velocity is recovered:

$$V_{inj} = \frac{1}{\rho_w} \sum_k \dot{s}_k \tag{8}$$

Equations (1) and (3) of the Hirschfleder and Curtiss approximation with correction velocity are then used to evaluate the normal diffusion flux of each species at the ablated wall:

$$Y_{k,w} V_{k,n} = -\mathcal{D}_k \frac{W_k}{W_w} \nabla_n X_{k,w} + Y_{k,w} V_n^{cor} \qquad \text{with} \qquad V_n^{cor} = \sum_k \mathcal{D}_k \frac{W_k}{W_w} \nabla_n X_{k,w} \tag{9}$$

Injecting Eq. (8) and Eq. (9) into Eq. (7), one can relate $Y_{k,w}$ to its normal gradient at the boundary surface:

$$-\mathcal{D}_k \nabla_n Y_{k,w} + Y_{k,w} \left(\frac{\sum_k \dot{s}_k}{\rho_w} + V_n^{cor} + W_w \mathcal{D}_k \sum_i \frac{\nabla_n Y_{i,w}}{W_i} \right) = \frac{\dot{s}_k}{\rho_w} \tag{10}$$

The explicit form of the latter equation gives the expression of $\nabla_n^{t+1} Y_{k,w}$ at time $t + \Delta t$ knowing the value of $Y_{k,w}^t$ at time t. Finally, the system Eq. (10) is solved with an iterative method and then, it is possible to prescribe the required values of the normal species gradients for each node at each time step. The tangential components of the species gradients are predicted by the scheme and left unchanged.

The temperature at the wall is imposed by using the same principle as for the inert wall case (see paragraph II.D.1). For the momentum equation, the normal velocity value is given by Eq. (8) while the tangential velocity components are set to zero.

Note that with the framework described above, no restriction is made for the number of chemical species or the number of chemical reactions involved in the pyrolysis process. Consequently, the boundary condition for ablated walls developed herein can be summarized through the following characteristics:

- arbitrary mixture and complex pyrolysis process can be considered,
- the variations of species concentrations is taken into account with a weak condition for $Y_{k,w}$,
- the ablative wall is sustained quasi-isothermal prescribing a weak condition for T_w,
- the velocity of pyrolysis gas is imposed with a Dirichlet condition for V_{inj}.

The key closure point of this boundary condition is the prescription of the species surface production rates $\dot{s}_k$. These closure values depend on the pyrolysis scheme retained to simulate the ablation behavior of a mixture/composite couple. For the application that motivates the present work, two heterogeneous reactions are usually retained to simulate the oxidation of C/C composites, namely:

$$C_{(s)} + H_2O \rightarrow H_2 + CO \tag{11}$$

$$C_{(s)} + CO_2 \rightarrow 2\, CO \tag{12}$$

Keswani and Kuo[22] have shown that H_2O is the dominant oxidizing species. As a consequence and for simplicity reason, the pyrolysis process is reduced to modeling the kinetics of Eq. (11) only.

The rate of progress $\mathcal{Q}$ (expressed in $mol \cdot m^{-2} \cdot s^{-1}$) of the retained equation can be formulated with an Arrhenius law:

$$\mathcal{Q} = \rho_w \frac{Y_{H_2O,w}}{W_{H_2O}}\, A\, T_w^{\beta}\, \exp\left(\frac{-E_a}{RT_w}\right) \tag{13}$$

where R is the perfect gas constant, A the pre-exponential constant, β the temperature exponent and E_a the activation energy. However, the empirical determination of the Arrhenius coefficients does not always provide sufficiently reliable results. For instance, the pre-exponential factor of the oxidation reactions of $C_{(s)}$ suggested by Golovina[23] are about an order of magnitude less than that of Libby and Blake.[24]

Since the ablation process is assumed to be quasi-isothermal, the use of the empirical terms of Eq. (13) can be rather replaced by the determination of a unique constant noted Ψ:

$$\mathcal{Q} = \rho_w \frac{Y_{H_2O,w}}{W_{H_2O}}\, \Psi \tag{14}$$

It is clear with the latter equation that the ablation process is governed by the diffusion of H_2O towards the walls. Moreover, the production rate of each species is expressed as:

$$\dot{s}_k = \nu_k W_k \mathcal{Q} \tag{15}$$

where ν_k is the difference between the backward and forward molar stoichiometric coefficients ($\nu_k = \nu_k^b - \nu_k^f$). Finally, replacing $\dot{s}_k$ of Eq. (8) by Eq. (15) with $\nu_{H_2} = \nu_{CO} = 1$ and $\nu_{H_O} = -1$, the relation between the constant factor Ψ of the heterogeneous reaction Eq. (11) and V_{inj} can be expressed:

$$\Psi = V_{inj} \frac{W_{H_2O}}{W_C} \frac{1}{Y_{H_2O,w}} \tag{16}$$

Hence, knowing the wall concentration of H_2O and imposing an injection velocity at the beginning of the DNS, it is possible to determine the value of Ψ that must be imposed all along the simulation. Consistently with available data in actual SRM, the value of Ψ for the present work has been set so that the injection velocity in viscous wall units at the beginning of the simulation is $V_{inj}^+ = 0.0035$.

The recession process of the solid surface implies geometrical changes of the simulation domain. However, the simulated time of the DNS being of oder $t_{simul.} \approx 10\ \tau_{diffusion} = 10\ h/u_\tau$ and with $V_{inj}^+ = 0.0035$, the relative variation of the channel half-width during the duration of the DNS is:

$$\frac{\Delta h}{h} \approx 10\ \frac{\dot{r}_c}{u_\tau} = 10\ \frac{\rho_w}{\rho_c}\ V_{inj}^+ \approx 0.01\% \tag{17}$$

Relatively to the width of the first cell at the wall, this corresponds to a variation of 3.7%. Consequently, it is considered that the recession surface does not move during the simulation which should not alter the statistics and which simplifies the numerical procedure.

III. Results and Discussion

In this section, first order statistics are assessed and results are analyzed comparing the statistics with the classical law of the wall and with the Artal and Nicoud[21] model able to take into account both the chemistry and non-unity Prandtl number effects. Mixture composition is also analyzed in terms of chemical equilibrium.

Inert Wall DNS Statistical Procedure

Instantaneous turbulent fields corresponding to the inert wall case have been averaged over space(for each plane parallel to the walls) and time (over 23 $\tau_{diffusion}$) to produce the statistics presented in the forthcoming paragraphs.

Ablated Wall DNS Statistical Procedure

Due to pyrolysis gas mass injection inside the computational domain, the DNS with ablation is not statistically steady. For instance, figure 2 shows the evolution of the mass fraction of H_2O and V_{inj}^+ during the simulation for a probing point at the wall. As a consequence, results concerning ablation are not averaged in time but only in space for an instantaneous solution; the statistics shown in the following correspond to space averaging at time $t_{simul.} = 5h/u_\tau = 5\ \tau_{diffusion}$ after the initialization of the DNS with ablation.

It is interesting to note in figure 2 that the operating condition $V_{inj}^+ = 0.0035$ (see table 3) is well matched at the beginning of the simulation. Moreover, the evolutions of the two probe parameters are closely similar: their values decrease quickly at the beginning of the simulation because the initial condition does not correspond to an ablative wall case. Hence, the retained observing time is $t_{simul.} = 5\ \tau_{diffusion}$ because this value is sufficient to eliminate this transient state occurring at the beginning of the simulation. This transient period is consistent with the pyrolysis model used into the ablated wall boundary condition. Indeed, Eq. (14) illustrates that the heterogeneous reaction is governed by the concentration of H_2O and thus by its diffusion towards the wall. Since the initial solution corresponds to an inert wall solution, the concentration of oxidizing species (i.e. H_2O in the present work) is higher than in an ablation configuration and the solution has to adapt before the diffusion of oxidizing species actually manages the ablation process.

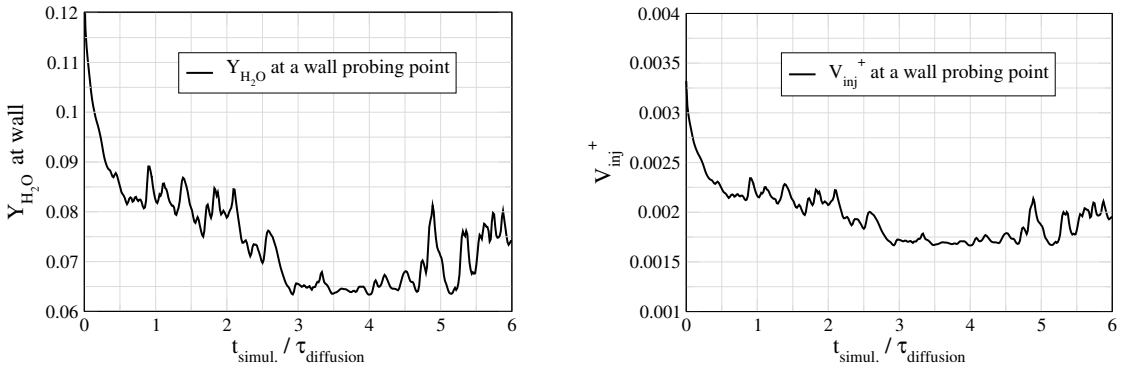

Figure 2. Evolution of the mass fraction of H_2O and V_{inj}^{+} during the simulation for a probing point at the wall.

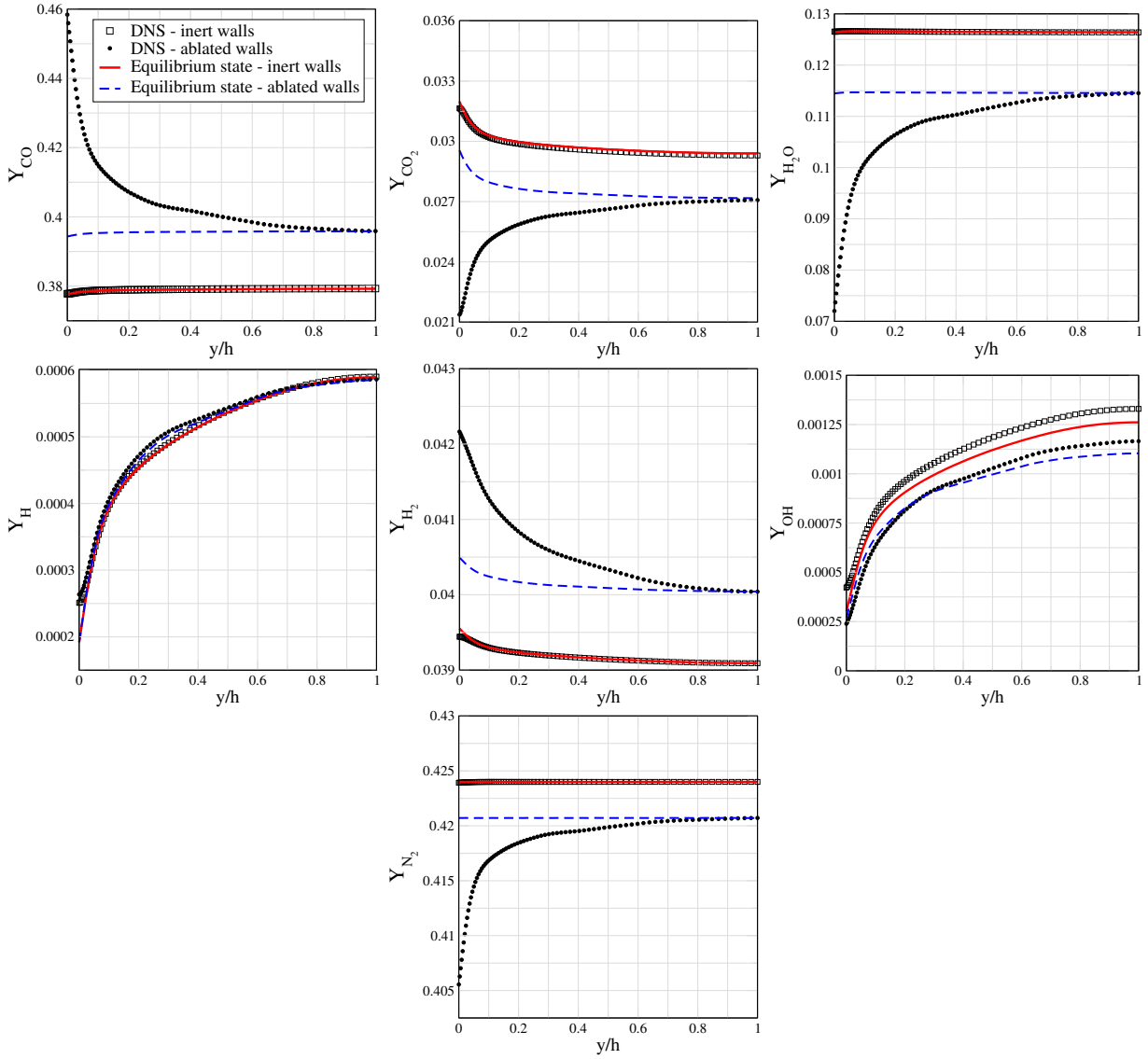

Figure 3. Mass fractions of the seven species involved in the simulated mixture. For both inert wall DNS and ablated wall DNS after $t_{simul.} = 5\ \tau_{diffusion}$, the chemical equilibrium states are assessed from CHEMKIN software using the composition of the mixture at $y = h$ and the DNS temperature profiles.

Considering the mixture composition at the center line of the computational domain, it is possible to assess if the assumption of chemical equilibrium is valid for the considered instantaneous ablation solution. To answer this question, figure 3 gathers the inert and ablation case concentration profiles confronted to the equilibrium state profiles obtained with the CHEMKIN software. The chemical equilibrium is evaluated for a constant pressure and temperature situation. Because the pressure inside the computation remains constant, the variation of the resulting profiles is solely due to the mean temperature profiles injected as inputs for the equilibrium characterization.

Figure 3 reveals that the equilibrium assumption is perfectly valid for multispecies inert wall modeling which is not true dealing with ablation. Thus, the development of reliable models for ablated walls requires another assumption to determine the composition of the mixture at the wall knowing the concentration of each species at a point situated further above the wall. Figure 3 also depicts that the error that could be made assuming a chemical equilibrium state is more apparent with species containing carbon which are more sensitive to the ablation process.

The statistic profiles of inert and ablation cases have been expressed in wall units and reported into figure 4. Simulation results are confronted to the classical law of the wall for velocity and temperature and with the Artal and Nicoud model whose development is presented in Ref. (21). This model has been specifically developed for velocity/temperature/chemistry coupled applications and is able to take into account the effects of variable molecular Prandtl number. It is based on the work of Kader[25] with the assumption of chemical equilibrium inside the boundary layer.

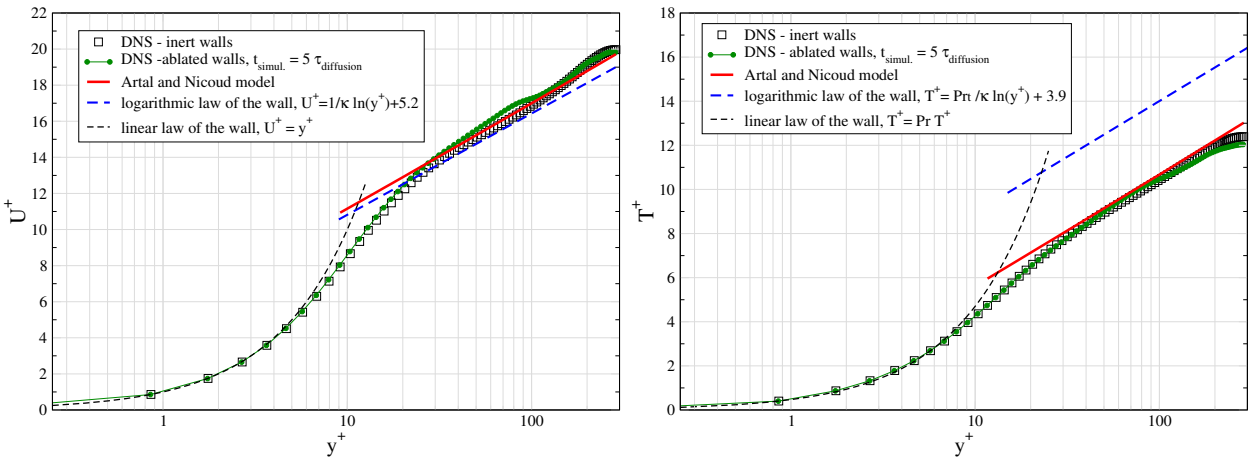

Figure 4. Dimensionless velocity (left) and temperature (right) profiles. Comparison between the inert wall DNS space and time averaged profile, the ablated DNS space averaged profile after simulation time $t_{simul.} = 5\ \tau_{diffusion}$, the Artal and Nicoud model and the classical law of the wall.

Figure 4 shows that the velocity profile is well recovered for both classical wall function and Artal and Nicoud model. However, the temperature profile is not well predicted with the classical law of the wall which is not a velocity/temperature coupled model. The prediction is clearly improved with the Artal and Nicoud model which is consistent with a chemical equilibrium assumption.

Moreover, for the considered ablation operating conditions, it appears that the heterogeneous reactions and the non-equilibrium state of the mixture does not influence the velocity and temperature profiles scaled in wall units.

IV. Conclusion and Future Work

DNS of periodic channel flow of a reacting mixture involving 7 species have been performed with and without heterogeneous reaction at the solid boundaries. The preliminary analysis performed so far indicates that classical wall functions for velocity and temperature are not accurate for assessing the momentum and heat flux at the boundary. Another formulation which accounts for large density gradients, non-unity Prandtl number and fast gaseous chemical reactions proves more accurate.

For the ablative case considered, the effect of wall ablation is not predominant. This behavior should not be observed with a stronger pyrolysis gas injection velocity.

Acknowledgments

The authors want to acknowledge the financial support and expertise of Snecma Propulsion Solide (SAFRAN group) as well as CNRS/DGA for the funding of first author's ongoing Ph.D. thesis. The authors are also grateful to CINES for the access to computing resources.

References

[1]Koo, J. H., Ho, D. W. H., and Ezekoye, O. A., "A Review of numerical and Experimental Characterization of Thermal Protection Materials - Part I. Numerical Modeling," *42nd AIAA/ASME/SAE/ASEE Joint Propulsion Conference and Exhibit*, Sacramento, California, 9-12 July 2006.

[2]Keswani, S. T. and Kuo, K. K., "An aerothermochemical model of carbon-carbon composite nozzle recession," *AIAA Paper 83-910*, 1983.

[3]Baiocco, P. and Bellomi, P., "A Coupled Thermo-Ablative and Fluid Dynamic Analysis for Numerical Application to Solid Propellant Rockets," *AIAA Paper 96-1811*, June 1996.

[4]Cai, T. and Hou, X., "Simple Method for Numerical Simulation of Temperature Response of the Solid Rocket Nozzle," *J. Thermophysics*, Vol. 4, Jan. 1990, pp. 42–46.

[5]Kendall, R. M., Rindal, R. A., and Bartlett, E. P., "A Multicomponent Boundary Layer Chemically Coupled to an Ablating Surface," *AIAA Journal*, Vol. 5, No. 6, 1967, pp. 1063–1071.

[6]Burakov, V. A. and Sandu, S. F., "Mathematical Modeling of the Dynamics of Slagging and Thermochemical Destruction of Carbon Composite Thermal Protective Materials in High-Temperature Two-Phase Flow," *Combustion, Explosion, and Shock Waves*, Vol. 33, No. 4, 1997, pp. 472–481.

[7]Wirzberger, H. and Yaniv, S., "Prediction of Erosion in Solid Rocket Motor by Alumina Particles," *AIAA Paper 2005-4496*, July 2005.

[8]Schönfeld, T. and Rudgyard, M., "Steady and Unsteady Flows Simulations Using the Hybrid Flow Solver AVBP," *AIAA Journal*, Vol. 37, No. 11, 1999, pp. 1378–1385.

[9]Colin, O. and Rudgyard, M., "Development of high-order Taylor-Galerkin schemes for unsteady calculations," *J. Comp. Physics*, Vol. 162, No. 2, 2000, pp. 338–371.

[10]Poinsot, T. and Veynante, D., *Theoretical and Numerical Combustion*, Edwards, 2005.

[11]Hirschfelder, J., Curtiss, F., and Bird, R., *Molecular theory of gases and liquids*, John Wiley & Sons, 1964.

[12]Giovangigli, V., *Multicomponent Flow Modeling*, Birkhäuser, 1999.

[13]Ern, A. and Giovangigli, V., *A General-purpose FORTRAN Library For Multicomponent Transport Property Evaluation*, CERMICS and CMAP, 2001.

[14]Geisler, R. L., "The Prediction of Graphite Rocket Nozzle Recession Rates," *the 1981 JANNAF Propulsion Meeting, New Orleans, LA*, Vol. 5, CPIA Publication 340, May 1981, pp. 173–196.

[15]Cvelbar, D. A., "Nozzle Recession Study," *the 1981 JANNAF Propulsion Meeting, New Orleans, LA*, CPIA Publication 342, May 1981, pp. 51–68.

[16]Keswani, S. T., Andiroglu, E., Campbell, J. D., and Kuo, K. K., "Recession behavior of graphitic nozzles in simulated rocket motors," *AIAA-1983-1317*, 1983.

[17]Kim, J., Moin, P., and Moser, R., "Turbulence statistics in fully developed channel flow at low Reynolds number," *Journal of Fluid Mechanics*, Vol. 177, No. 133-166, 1987.

[18]Moser, R., Kim, J., and Mansour, N., "Direct numerical simulation of turbulent channel flow up to $\mathrm{Re}_\tau = 590$," *Physics of Fluids*, Vol. 11, No. 4, 1999, pp. 943–945.

[19]Hoyas, S. and Jiménez, J., "Scaling the velocity fluctuations in turbulent channel up to $\mathrm{Re}_\tau = 2003$," *Physics of Fluids*, Vol. 18, No. 011702, 2006, pp. 18–21.

[20]Jiménez, J. and Moin, P., "The minimal flow unit in near-wall turbulence," *Journal of Fluid Mechanics*, Vol. 225, No. 213-240, 1991.

[21]Artal, L. and Nicoud, F., "Direct Numerical Simulation of Reacting Turbulent Multi-species Channel Flow," *In Proceedings of the 6th ERCOFTAC Workshop - Direct and Large-Eddy Simulation*, Poitiers, France, 2005, pp. 381–388.

[22]Keswani, S. T. and Kuo, K. K., "Validation of an Aerothermochemical model for Graphite Nozzle Recession and Heat-Transfer Process," *Combust. and Tech.*, Vol. 47, 1986, pp. 177–192.

[23]Golovina, E. C., "The Gasification of Carbon by Carbon dioxyde at High Temperatures ans Pressures," *Carbon*, Vol. 18, 1980, pp. 197–201.

[24]Libby, P. A. and Blake, T. R., "Theoretical Study of Burning Coal Particles," *Combustion and Flame*, Vol. 36, 1979, pp. 139–169.

[25]Kader, B. A., "Temperature and Concentration Profiles in Fully Turbulent Boundary Layers," *Journal of Heat and Mass Transfer*, Vol. 24, No. 9, 1981, pp. 1541–1544.